Biomed Microdevices (2016) 18:108
DOI 10.1007/s10544-016-0134-3

Ethosomes and organogels for cutaneous administration of crocin

Elisabetta Esposito[1] · **Markus Drechsler**[2] · **Nicolas Huang**[3] · **Gabriella Pavoni**[1] · **Rita Cortesi**[1] · **Debora Santonocito**[4] · **Carmelo Puglia**[4]

Abstract The present study describes the production and characterization of phosphatidylcholine based ethosomes and organogels, as percutaneous delivery systems for crocin. Crocin presence did not influence ethosome morphology, while the drug slightly increased ethosome mean diameter. Importantly, the poor chemical stability of crocin has been found to be long controlled by organogel. To investigate the performance of phosphatidylcholine lipid formulations as crocin delivery system, *in vivo* studies, based on tape stripping and skin reflectance spectrophotometry, were performed. Tape stripping results suggested a rapid initial penetration of crocin exerted by the organogel, probably due to a strong interaction between the peculiar supramolecular aggregation structure of phospholipids in the vehicle and the lipids present in the stratum corneum and a higher maintenance of crocin concentration in the case of ethosomes, possibly because of the formation of a crocin depot in the stratum corneum. Skin reflectance spectrophotometry data indicated that both vehicles promoted the penetration of crocin through the skin, with a more rapid anti-inflammatory effect exploited by ethosomes, attributed to an ethanol pronounced penetration enhancer effect and to the carrier system as a whole.

Keywords Phospholipid · Nanotechnology · Viscosity · Chemical stability · Permeation enhancers

Abbreviations

ETHO	Ethosomes
ORG	Organogels
CRO	Crocin
X GUM	Xanthan gum
PC	Phosphatidylcholine
MED	Minimal erythemal dose

1 Introduction

Bioactive natural components, such as phytochemicals derived from edible plants, are effective in preventing or suppressing the process of carcinogenesis and other chronic diseases (Weng and Yen 2012). For instance polyphenols, flavonoids, isoflavonoids, proanthocyanidins, phytoalexins, anthocyanidins and carotenoids have been recognized as potential skin cancer chemopreventive agents (Mittal et al. 2003; Surh 2003; Nandakumar et al. 2008; Meeran et al. 2009; Weng and Yen 2012). Moreover many of them are under clinical study, being able to interfere with specific stages of the carcinogenic process (Wanga et al. 2012). Skin carcinogenesis is a multistep process which consists in malignant

Electronic supplementary material The online version of this article (doi:10.1007/s10544-016-0134-3) contains supplementary material, which is available to authorized users.

✉ Elisabetta Esposito
ese@unife.it

✉ Rita Cortesi
crt@unife.it

[1] Department of Life Sciences and Biotechnologies, University of Ferrara, I-44121 Ferrara, Italy

[2] Macromolecular Chemistry II, University of Bayreuth, Bayreuth, Germany

[3] Institut Galien Paris-Sud (CNRS UMR 8612), Faculté de Pharmacie, Université Paris-Sud, Orsay, France

[4] Department of Drug Science, University of Catania, I-95125 Catania, Italy

Published online: 10 November 2016

growth of the epidermis induced by chemical carcinogens or UV irradiation, generating reactive oxygen species (Robertson 2012). In this respect cellular antioxidant and cytoprotective proteins can protect against skin carcinogenesis (Chun et al. 2014).

Crocin (CRO), the diester of the disaccharide gentiobiose and the dicarboxylic acid crocetin, is a carotenoid compound responsible for the colour of saffron, occurring naturally in crocus and gardenia fruit (Winterhalter and Straubinger 2000). Due to its powerful antioxidant properties, CRO could be useful in a number of pathologies, i.e. neurodegenerative disorders, atherosclerosis, depression and liver diseases (Alavizadeh and Hosseinzadeh 2014). In addition CRO exerts significant antinociceptive and anti-inflammatory activity, as well as chemopreventive and anti-cancer properties, as suggested by different studies (Escribano et al. 1996; Konoshima et al. 1998).

Unfortunately, CRO is scarcely stable, indeed it loses most of its functionality after exposure to heat, oxygen, light and acids (Tsimidou and Tsatsaroni 1993). Moreover it has been demonstrated that CRO has poor absorption and low bioavailability after oral administration, being hydrolyzed by β-glucosidase and rapidly eliminated (Asai et al. 2005). Thus, despite its beneficial effects, CRO chemical instability and high susceptibility to process conditions represent obstacles for its therapeutic application.

In the present study, in an attempt to design topical vehicles for CRO able to improve its stability, different phosphatidylcholine based nano-systems, such as ethosomes (ETHO) and organogels (ORG), have been considered.

Phosphatidylcholine (PC), a versatile natural and biocompatible surfactant, is able to form a number of supra-molecular structures (i.e. direct and inverted micelles or hexagonal, cubic and lamellar phases), providing the opportunity to produce innovative (trans)dermal forms (Grdadolnik et al. 1991). Indeed due to its affinity with skin lipids, PC can exert penetration enhancer properties, increasing skin permeation (Wohlrab et al. 2010; Tian et al. 2012).

ETHO can be defined as lipid vesicular systems constituted of phospholipids (such as soy PC), ethanol and water. ETHO find interesting application as percutaneous delivery systems. Indeed the presence of ethanol in high concentrations (20–45 %) confers to ETHO a soft structure which promotes enhancer delivery to/through the skin (Touitou et al. 2000). The penetration enhancement mechanisms of ETHO should be ascribed to fusion with skin lipids, as well as to penetration of intact ETHO, as a function of ETHO composition and physical characteristics (Godin and Touitou 2003; Jain et al. 2007).

ORG are gel-like reverse micellar systems in which PC is solubilized in a biocompatible oil (Raut et al. 2012). Particularly, the addition of a precise amount of water to a PC oil solution initially leads to production of spherical reversed micelles, afterwards the micellar aggregates intertwine, forming a three-dimensional network in the bulk phase. Their peculiar structure and the possibility to modulate the system viscosity make ORG suitable for (trans)cutaneous administration of hydrophilic and lipophilic molecules (Patil et al. 2011; Esposito et al. 2013).

In the present investigation, the efficiency of ETHO and ORG as cutaneous delivery systems for CRO has been studied.

Notably, the capability of ETHO and ORG to control CRO stability has been investigated.

Special regard has been devoted to an *in vivo* investigation aimed to study CRO amount in *stratum corneum* and CRO anti-inflammatory activity after cutaneous application.

2 Materials and methods

2.1 Materials

Crocin (CRO, crocetin digentibiose ester), xanthan gum (X GUM) and isopropylpalmitate were purchased from Sigma Chemical Company (St Louis, MO, USA). The soybean lecithin (PC) (90 % phosphatidylcholine) used for ETHO and ORG preparation was Epikuron 200 from Lucas Meyer, Hamburg, Germany. Solvents were of HPLC grade and all other chemicals were of analytical grade.

2.2 Production of ethosomes

For the preparation of ETHO, PC (30 mg/ml) was first dissolved in ethanol (30 %, *v/v*). Afterwards isotonic Palitzsch buffer (IPB) (5 mM $Na_2B_40_7$, 180 mM H_3BO_3, 18 mM NaCI), was slowly added to the ethanolic solution under continuous stirring at 700 rpm by an IKA Eurostar digital (IKA Labortechnik Janke & Kunkel, Staufen, Germany). Mechanical stirring was performed for 30 min at room temperature in the dark. In the case of CRO containing ETHO (ETHO-CRO), CRO (0.5 mg/ml) was added to IPB before addition to PC ethanol solution. Table 1 reports the ETHO composition.

In order to obtain homogeneously sized vesicles, ETHO-CRO were subjected to two extrusion cycles through 400 nm pore size polycarbonate filters.

2.3 Characterization of ethosomes

2.3.1 Cryo-Transmission Electron Microscopy (Cryo-TEM)

Samples were vitrified as described in a previous study (Esposito et al. 2012). Briefly a sample droplet of 2 uL was put on a lacey carbon filmed copper grid (Science Services, Muenchen) for 30 s. Subsequently, most of the liquid was

Table 1 Composition of formulations employed in this study

Formulations	Soy phosphatidylcholine *% w/w*	Ethanol *% w/w*	Isopropyl palmitate *% w/w*	Crocin *% w/w*	Aqueous phase[a] *% w/w*
ETHO	3.0	27.0	–	–	70.00 (IPB)[a]
ETHO-CRO	3.0	27.0	–	0.05	69.50 (IPB)[a]
ORG	14.7	–	85.12	–	0.18 (water)
ORG-CRO	14.7	–	85.12	0.05	0.13 (water)

[a] isotonic Palitzsch buffer

removed with blotting paper leaving a thin film stretched over the lace holes. The specimens were instantly shock frozen by rapid immersion into liquid ethane cooled to approximately 90 K by liquid nitrogen in a temperature-controlled freezing unit (Zeiss Cryobox, Carl Zeiss Microscopy GmbH, Jena, Germany). The temperature was monitored and kept constant in the chamber during all the sample preparation steps. After freezing the specimens, the remaining ethane was removed using blotting paper. The vitrified specimen was transferred to a Zeiss/Leo EM922 Omega EFTEM (Zeiss Microscopy GmbH, Jena, Germany) transmission electron microscope using a cryoholder (CT3500, Gatan, Munich, Germany). Sample temperature was kept below 100 K throughout the examination. Specimens were examined with reduced doses of about 1000–2000 e/nm^2 at 200 kV. Images were recorded by a CCD digital camera (Ultrascan 1000, Gatan, Munich, Germany) and analysed using a GMS 1.9 software (Gatan, Munich, Germany).

2.3.2 Photon Correlation Spectroscopy (PCS)

Submicron particle size analysis was performed using a Zetasizer 3000 PCS (Malvern Instr., Malvern, England) equipped with a 5 mW helium neon laser with a wavelength output of 633 nm. Glassware was cleaned of dust by washing with detergent and rinsing twice with sterile water. Measurements were made at 25 °C at an angle of 90° with a run time of at least 180 s. Samples were diluted with bidistilled water in a 1:10 v:v ratio. Data were analysed using the "CONTIN" method (Pecora 2000). Measurements were performed in triplicate on freshly prepared samples and after 6 months from production.

2.4 CRO content of ethosomes

The entrapment capacity (EC) of CRO in ETHO was determined (Touitou et al. 2000). 100 μl aliquot of ETHO-CRO was loaded in a centrifugal filter (Microcon centrifugal filter unit YM-10 membrane, NMWCO 10 kDa, Sigma Aldrich, St Louis, MO, USA) and centrifuged (Spectrafuge™ 24D Digital Microcentrifuge, Woodbridge NJ, USA) at 8,000 rpm for 20 min. The amount of free and entrapped CRO was determined by dissolving the supernatant with a known amount of ethanol (1:10, *v/v*). The amount of CRO in the supernatant was determined by high performance liquid chromatography (HPLC) method, as below reported. The EC was determined as follows:

$$EC = T_{CRO} - S_{CRO}/T_{CRO} \times \quad 100 \tag{1}$$

where T_{CRO} stands for the total amount of CRO added to the formulation and S_{CRO} for the amount of drug measured in the supernatant.

2.5 Production of organogels

Production of ORG was conducted by adding precise amounts of water to PC (200 mM) solution in isopropylpalmitate, under stirring. The amount of added water has been expressed as the molar water to PC ratio ([water]/[PC]) (Schipunov 2001). $[Water]/[PC]_{max}$ was determined, i.e. the highest amount of water that can be incorporated into the PC solution with no phase separation. The samples were maintained under stirring at 25 ° C for 30 min and later examined under a Leitz diaplan microscope (Lietz Wetzlar, Germany) equipped with a polarizer positioned in the light pass before the specimen.

To produce CRO containing ORG (ORG-CRO), CRO was previously solubilized in water before addition to PC solution. CRO final concentration in ORG-CRO was 0.05 *% w/v*. Table 1 reports the ORG composition.

2.6 Prediction of long-term stability

The stability of CRO was assessed in aqueous solution, ETHO-CRO and ORG-CRO stored in glass containers at 25 °C for 3 months.

Chemical stability was evaluated, determining CRO content by HPLC analyses. Shelf life values were calculated as below reported (Pugh 2007).

Log (CRO residual content, %) was plotted against time and the slopes (m) were calculated by linear regression.

The slopes (m) were then substituted into the following equation for the determination of k values:

$$k = m \times 2.303 \tag{2}$$

Shelf life values (the time for 10 % loss, t_{90}) and half-life (the time for 50 % loss, $t_{1/2}$) were then calculated by the following equations:

$$t_{90} = 0.105/k \quad (3)$$

$$t_{1/2} = 0.693/k \quad (4)$$

2.7 Gel production

Ethosome viscosity has been improved by adding x-gum (1 % *w/w*) directly into the dispersion and by slowly stirring for 1 h until complete dispersion of the gum. The obtained viscous ETHO formulation has been named ETHO-CRO X-GUM.

2.8 Rheological measurements

Rheological measurements were performed with an AR-G2 rotational rheometer (TA Instruments). The geometry used was an aluminium cone-plate with a diameter of 40 mm and an angle of 1°. Flow curves were obtained by increasing the shear rate from 0.01 to 5000 s^{-1} with 5 points per decade, each point was maintained for a duration of 180 s in order to perform measurements in the permanent regime. The temperature was set at 25 °C or 35 °C and controlled with a Peltier plate. A solvent trap was used to prevent water evaporation. Measurements were performed in triplicate for each sample, to ensure reproducibility.

2.9 *In vivo* studies

2.9.1 Volunteers recruitment

In vivo experiments were performed on two groups of ten volunteers: group A enrolled for the first *in vivo* experimentation (tape-stripping) and group B enrolled for the second one (evaluation of anti-inflammatory activity).

Experiments were conducted in accordance with The Code of Ethics of the World Medical Association (Helsinki Declaration 1964) and its later amendments for experiments involving humans.

The volunteers were of both sexes in the age range 25–55 years and recruited after medical screening including the filling of a health questionnaire followed by physical examination of the application sites. Informed consent was obtained from all individual participants included in the study. The participants did not suffer from any ailment and were not on any medication at the time of the study. They were rested for 15 min prior to the experiments and room conditions were set at 22 ± 2 °C and 40–50 % relative humidity.

2.9.2 Tape Stripping

For each subject (group A), ten sites on the ventral surface of each forearm were defined using a circular template (1 cm^2) and demarcated with permanent ink. One of the ten sites of each forearm was used as control, three sites were treated with 300 mg of ETHO-CRO-X GUM, three sites were treated with 300 mg of ORG-CRO and the remaining three with 300 mg of X GUM-CRO. The preparations were spread uniformly by means of a solid glass rod and then the sites were occluded for 6 h using Hill Top Chambers (Hill Top Research, Cincinnati, OH). After the occlusion period, the residual formulations were removed by gently wiping with cotton balls (different for each pretreated site). Ten individual 2 cm^2 squares of adhesive tape (Scotch Book Tape 845, 3M) were utilized to sequentially tape-strip the *stratum corneum* on the application sites. The removal of *stratum corneum* in each pretreated site was effected at 1 h (t = 1), 3 h (t = 3) and 6 h (t = 6) after formulation removal (Esposito et al. 2014).

Each adhesive square, before and after skin tape stripping, was weighed on a semi-micro balance (sensitivity 1 mg, Sartorius model ME415S, Goettingen, Germany) to quantify the weight of removed *stratum corneum*. After each stripping, the tapes were put in the same vial containing 2 ml of the HPLC mobile phase methanol:water (65:35 *v/v*) and subjected to vortical stirring over 30 s. The extracted CRO was then quantified by HPLC. The recovery of CRO was validated by spiking tape-stripped samples of untreated *stratum corneum* with 2 ml of a mobile phase containing CRO 10 mg/ml. The extraction efficiency of CRO was 97.2 ± 0.5 % ($n = 3$).

2.9.3 In vivo anti-inflammatory activity

The *in vivo* anti-inflammatory activity has been evaluated by measuring the inhibition of the UVB-induced skin erithema. In particular, the UVB-induced skin erythema was monitored by using a reflectance visible spectrophotometer X-Rite model 968 (XRite Inc. Grandville, MI, USA), calibrated and controlled as previously reported (Esposito et al. 2005). Reflectance spectra were obtained over the wavelength range 400–700 nm using illuminant C and 2° standard observer. From the spectral data obtained, the erythema index (EI) was calculated using Eq. (5).

$$E.I. = 100\left[\log\frac{1}{R_{560}} + 1.5\left(\log\frac{1}{R_{540}} + \log\frac{1}{R_{580}}\right) - 2\left(\log\frac{1}{R_{510}} + \log\frac{1}{R_{610}}\right)\right] \quad (5)$$

where 1/R is the inverse reflectance at a specific wavelength (560, 540, 580, 510 and 610). The skin erythema was induced by UVB irradiation using a UVM-57 ultraviolet lamp (UVP, San Gabriel, CA, USA) ultraviolet lamp emitting in 290–320 nm range, with 302 nm output peak, the rate measured

at the skin surface was 0.80 mW/cm^2. The minimal erythemal dose (MED) was preliminarily determined, and an irradiation dose corresponding to twice the value of MED was used throughout the study. For each subject (group B), seven sites on the ventral surface of each forearm were defined using a circular template (1 cm^2) and demarcated with permanent ink. One of the seven sites of each forearm was used as control, three sites were treated with 300 mg of ETHO-CRO-X GUM and the remaining three with 300 mg of ORG-CRO. The preparations were spread uniformly by means of a solid glass rod and then the sites were occluded for 6 h using Hill Top Chambers (Hill Top Research, Cincinnati, OH). After the occlusion period, the chambers were removed and the skin surfaces were gently washed and allowed to dry for 15 min. Each pre-treated site was exposed to UV-B irradiation 1, 3 and 6 h (t = 1, t = 3 and t = 6, respectively) after ETHO-CRO-X GUM and ORG-CRO removal and the induced erythema was monitored for 52 h. EI baseline values were taken at each designated site before application of gel formulation and they were subtracted from the EI values obtained after UV-B irradiation at each time point to obtain ΔEI values. For each site, the AUC was computed using the trapezoidal rule. To better outline the results obtained, the PIE (percentage of inhibition of erythema) was calculated from the AUC values using Eq. (6):

$$\text{Inhibition}(\%) = \frac{\text{AUC}_{(C)} - \text{AUC}_{(T)}}{\text{AUC}_{(C)}} \times 100 \quad (6)$$

where $\text{AUC}_{(C)}$ is the area under the response/time curve of the vehicle-treated site (control) and $\text{AUC}_{(T)}$ is the area under the response/time curve of the drug-treated site.

2.9.4 Statistical Analysis

Statistical differences of *in vivo* data were determined using repeated-measures analysis of variance (ANOVA) followed by the Bonferroni-Dunn post hoc pairwise comparison procedure. The employed software was Prism 5.0, Graph Pad Software Inc. (La Jolla, CA - USA). A probability of less than 0.05 is considered significant in this study.

2.10 HPLC Procedure

HPLC determinations were performed using a quaternary pump (Agilent Technologies 1200 series, USA) an UV-detector operating at 440 nm, and a 7125 Rheodyne injection valve with a 50 μl loop. Samples were loaded on a stainless steel C-18 reverse-phase column (15 × 0.46 cm) packed with 5 μm particles (Grace® - Alltima, Alltech, USA).

Elution was performed with a mobile phase containing methanol:water (65:35, *v/v*) at a flow rate of 0.8 ml/min, retention time was 4.5 min. The method was validated for linearity ($R_2 = 0.995$), repeatability (relative standard deviation 0.01 %, $n = 6$ injections) and limit of quantification (0.04 μg/ml).

3 Results

3.1 Preparation and characterization of ethosomes

Production of ETHO was spontaneously obtained by slow addition of an aqueous buffer to a PC ethanol solution under continuous stirring at room temperature. The presence of ethanol allowed to solubilize PC and to confer initial optical transparency to the dispersion. The addition of IPB buffer resulted in an increase of turbidity, suggesting the formation of ethosomal vesicles. In the case of CRO containing ETHO, the presence of the drug conferred a yellow colour to the dispersion (as shown in Online Resource 1 A).

The morphological analysis of ETHO investigated by cryo-TEM, shown in Fig. 1, revealed the presence of multilamellar spherical vesicles and multivesicular vesicles, both in the case of ETHO (Fig. 1a, b) and ETHO-CRO (Fig. 1c, d). At the highest magnification the presence of a double layer in ETHO vesicle conformation can be observed (Fig. 1b, d).

Table 2 summarizes the dimensional distribution of ETHO dispersions obtained by PCS analysis. Vesicle mean diameter was 332 and 454 nm in the case of ETHO and ETHO-CRO, respectively. Particularly vesicles were characterized by a bimodal dimensional distribution (PI 0.32 and 0.38). The presence of CRO slightly increased both mean diameter and polydispersity of vesicles. In order to obtain homogeneous monolamellar vesicles, ETHO-CRO vesicles have been extruded through polycarbonate membranes with calibrated pores (400 and 200 nm), this strategy led to a decrease of mean diameter up to 250 nm, PI 0.28.

After 6 months from production, mean diameters underwent a 48 or 18 % increase in the case of ETHO and ETHO-CRO respectively.

3.2 Preparation of organogels

Production of ORG was conducted by adding precise amounts of water to reverse micellar solutions constituted of PC solubilized in isopropylpalmitate. After 30 min of magnetic stirring, transparent gels were obtained, whose consistency was a function of the amount of added water (as shown in Online Resource 1 B). Particularly 1:1, 2:1 and 3:1 [water]/[PC] ratio have been considered (Online Resource 1 B). (Luisi et al. 1990). Since the $[\text{water}]/[\text{PC}]_{max}$ was found to be 3:1, the corresponding amount of water was selected for ORG and ORG-CRO production. Both ORG and ORG-CRO were transparent, yellow, macroscopically monophasic and isotropic under polarized light.

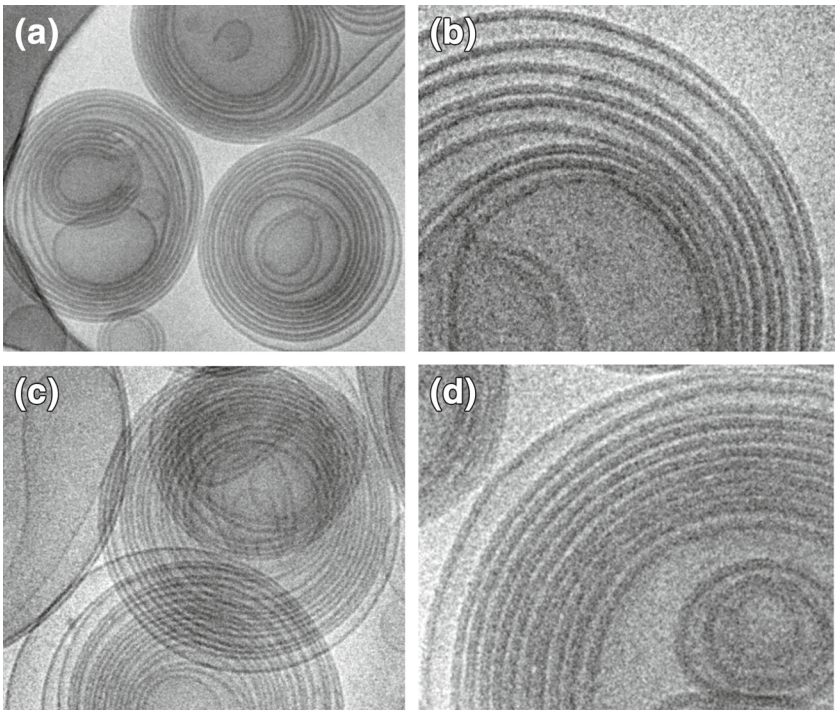

Fig. 1 Cryo-transmission electron microscopy images (cryo-TEM) of ETHO (**a**, **b**) and ETHO-CRO (**c**, **d**). Bar corresponds to 200 or 85 nm in panels **a**, **c** and **b**, **d** respectively

3.3 Entrapment capacity (EC)

The preparation of ETHO-CRO and ORG-CRO was spontaneously performed at 25 °C under magnetic stirring in dark vials, preventing drug loss on mechanical devices, as well as thermal or light degradation. For this reason, it was reasonable to obtain almost quantitative recovery of drug into the formulations.

Nonetheless it should be considered that in the case of ORG-CRO, being constituted of reverse micelles, CRO was entrapped inside the micelles in the aqueous environment, while in the case of ETHO-CRO, CRO was expected to be dissolved partly inside the vesicles and partly within the aqueous environment out of the vesicles (Fig. 2). Therefore, the ultracentrifugation method was employed in order to calculate the EC (Touitou et al. 2000).

The obtained data indicate that CRO inside the vesicles was 74 %, while the amount of CRO out of the vesicle was 26 % (Table 3).

It should be underlined that the strategy of extruding ETHO-CRO resulted in a loss of the drug. Indeed the extrusion process led to an escape of CRO, finally resulting in a 48 ± 3 % EC value for ETHO-CRO. For this reason ETHO-CRO have been employed for *in vivo* studies as they were.

For *in vivo* experiments CRO amount in ETHO-CRO and in ORG-CRO was the same, because unentrapped CRO was not separated from ETHO-CRO vesicles.

3.4 Crocin stability

CRO content in ETHO-CRO and ORG-CRO was determined as a function of time and expressed as percentage of the total amount used for the preparation (Fig. 3). It is evident that the degradation of CRO was more controlled by ORG-CRO than by ETHO-CRO, indeed CRO residual content after 3 months was 78 and 30 %, respectively. Conversely CRO solution was almost completely degraded after 15 days.

Table 2 Dimensional parameters of ethosomes as determined by PCS

Formulations	Z average Size (nm)	Polydispersity index	Typical Intensity distribution		
			peak	nm	area %
ETHO	332.1 ± 20	0.32 ± 0.03	1	440	26
	(492.2 ± 40)[a]	(0.29 ± 0.08)[a]	2	162	74
ETHO-CRO	454.0 ± 32	0.38 ± 0.05	1	850	7
	(534.0 ± 50)[a]	(0.37 ± 0.15)[a]	2	253	93

[a] after 6 months from production

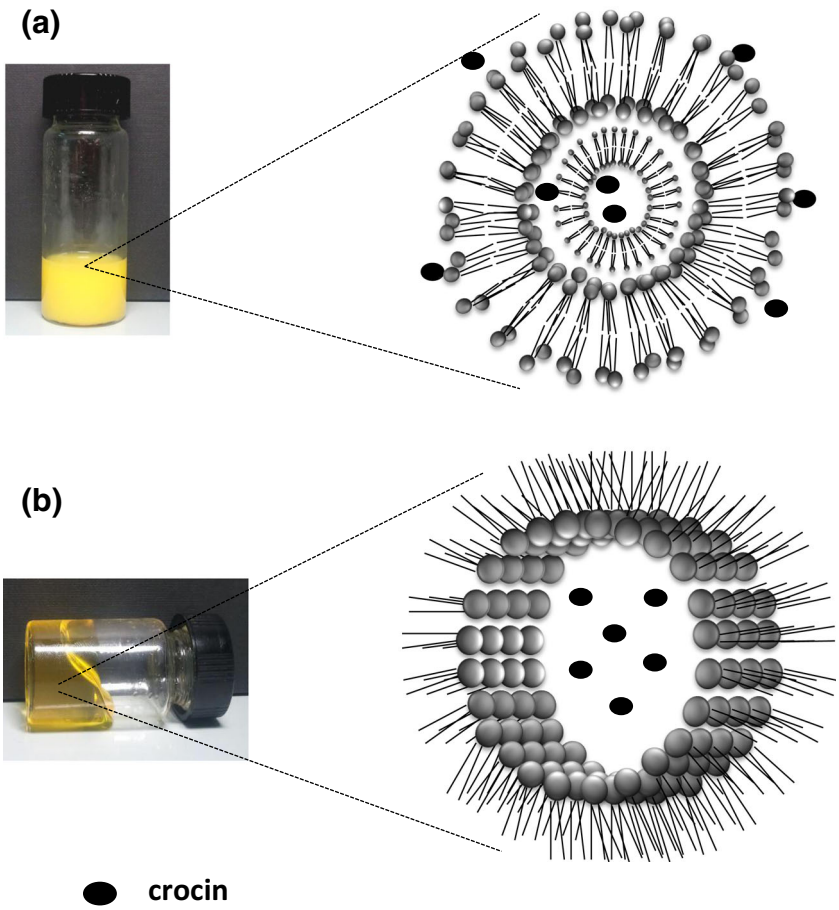

Fig. 2 Photographs and schematic drawings of ETHO-CRO (**a**) and ORG-CRO (**b**). In particular in panel **a** is drawn the possible distribution of CRO (●) in the aqueous environment inside and outside ETHO-CRO vesicles, while in the case of ORG-CRO (**b**) CRO is mainly located in the aqueous domain inside the reverse micelles

Table 3 reports shelf life (t_{90}) and half life ($t_{1/2}$) values calculated by Eqs. (3) and (4).

It was found that ORG could maintain 90 % of CRO stability for almost 38 days, whilst in the case of ETHO, t_{90} was 7 days. The $t_{1/2}$ values reached almost 8 months in the case of ORG-CRO, and 2 months in the case of ETHO-CRO. All data were statistically significant ($p < 0.0001$).

Nevertheless both ETHO-CRO and ORG-CRO did not show changes in physical appearance by time, maintaining homogeneous aspect, absence of phase separation phenomena and/or aggregates also after 6 months from production.

Table 3 Entrapment capacity and shelf life values of ethosomes and organogels

Formulations	EC[a] %	m[b]	K[c]	t_{90}(days) [c]	$t_{1/2}$(days) [c]
CRO solution	n.d.	0.133	0.306	0.34	2.26
ETHO-CRO	74.44 ± 3.5	0.0063	0.014	7.13	47.14
ORG-CRO	99.5 ± 0.5	0.0012	0.002	37.75	236.51

[a] EC: entrapment capacity

[b] slope of the line of log(CRO residual content %) kinetic, calculated as the mean of 3 independent determinations, s.d. ≤ 5 %

[c] K, t_{90} and $t_{1/2}$ were calculated following Eqs. 2, 3 and 4 respectively

3.5 Gelation of ethosomes and rheological analyses

ORG-CRO with 3:1 [water]/[PC] ratio is characterized by a suitable viscosity for cutaneous administration (8.03 ± 0.3 Pa.s

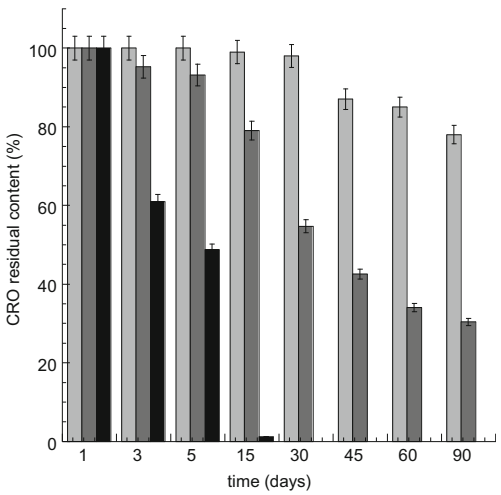

Fig. 3 Variation of CRO residual content in ETHO-CRO (*grey*), ORG-CRO (*light grey*) and CRO aqueous solution (*black*) as a function of time. The formulations were stored in glass containers at 25 °C for 3 months. Data are the means of 5 analyses on different batches of the same type of formulations. Standard deviations were comprised between ± 5 %

at 25 °C, shear rate 10 s^{-1}). Instead, the low viscosity of ETHO-CRO, did not enable its topical application, for this reason X GUM was directly added into ETHO dispersion. The resulting ETHO-CRO-X GUM possessed a viscosity adequate for cutaneous administration, being 2.72 ± 0.2 Pa.s at 25 °C, shear rate 10 s^{-1}.

Figure 4 shows flow curves for ETHO-CRO-X GUM (A), ORG-CRO (B) and CRO-X GUM (C). In particular the viscosity vs. shear rate has been measured at 25 °C (grey profile) and 35 °C (black profile), in order to mimic storage condition or skin application, respectively. The points on the curves are the means of three experiments and error bars represent standard deviation. All samples were very slightly thixotropic, indeed the upward and down curves are almost superimposed.

In Fig. 4a and c, flow curves exhibit a marked non-Newtonian shear thinning behavior: the steady shear viscosity sharply decreased as an increase in shear rate. In addition, the first and second Newtonian plateaux are not observed at low and high shear rates respectively. The temperature did not influence the behaviour of the material, in fact the curves at 25 °C or 35 °C are superimposable.

In Fig. 4b ORG-CRO shows an initial Newtonian plateau at both temperature followed by a shear thinning behaviour: the Newtonian plateau extends from 0.01 to 2 s^{-1} (at 25 °C) or 10 s^{-1} (at 35 °C), and the viscosity decreases significantly after the Newtonian plateaux. Indeed, the shear is then high enough to break significantly the structure of the gel (shear thinning behaviour) and, above 200 s^{-1} , to conceal the effect of temperature.

Below 200 s^{-1}, the viscosity is higher at 25 °C than at 35 °C, with a difference of one order of magnitude at the Newtonian plateaux. The second Newtonian plateau can't be observed, even at the maximum shear rate of the experiment: the microscopic structure of the material could be possibly modified at higher shear rate.

Flow curves of ETHO, ORG and X GUM are not shown since they are superimposable to the reported curves. Indeed, the presence of CRO did not influence the viscosity of the material.

3.6 Tape-stripping evaluation

The tape stripping experiment was employed for quantifying drug presence in the viable epidermis and the amount of CRO responsible for the anti-inflammatory effect (Esposito et al. 2005, 2014). Formulations have been applied and removed from the forearms as depicted in the scheme of Fig. 5a. From the analysis of the data reported in Fig. 5b, both ETHO-CRO-X GUM and ORG-CRO induced a depletion in the amount of CRO in the stratum corneum. Notably in the case of ORG-CRO the depletion was more intense, indeed after 1, 3 and 6 h the amount of CRO was 1/2, 1/3 and 1/6 with respect to ETHO-CRO-X GUM. Contrarily, in the case of X GUM-CRO, CRO amount was nearly the same all over the period after formulation removal. Importantly the amounts of CRO recovered in the stratum corneum after removal of ETHO-

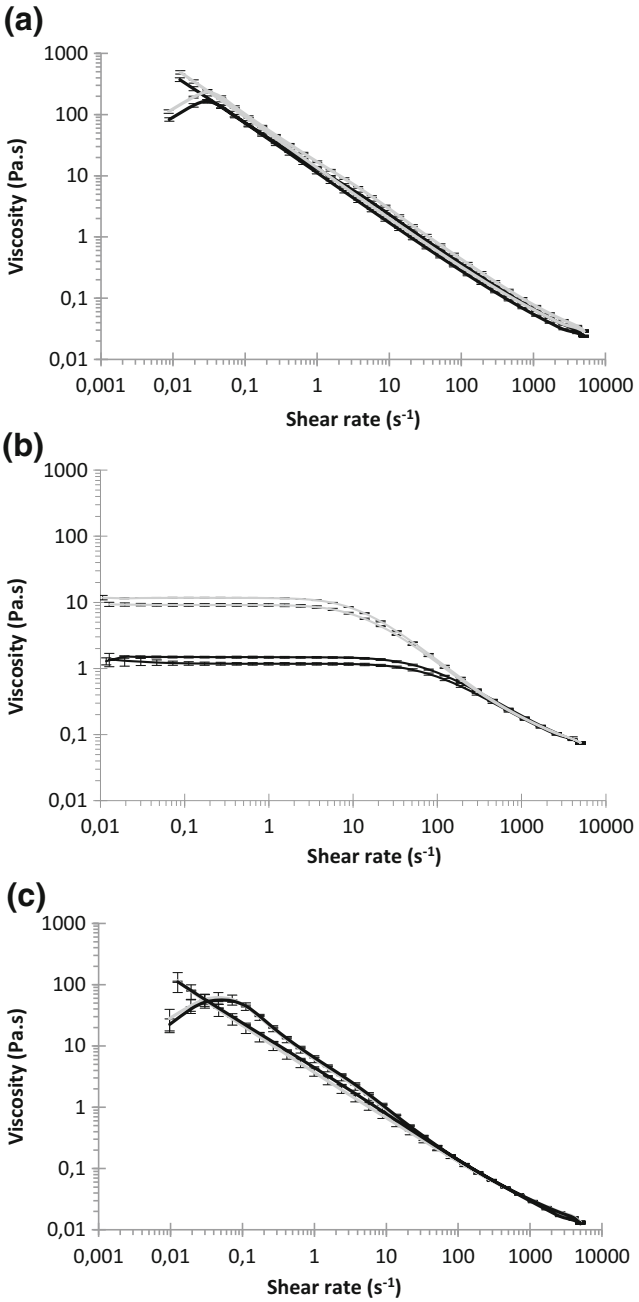

Fig. 4 Rheological flow curves for ETHO-CRO-X GUM (**a**), ORG-CRO (**b**) and X GUM (**c**), determined at 25 (*grey line*) and 35 °C (*black line*). The geometry used was an aluminium cone-plate. Flow curves were obtained by increasing the shear rate from 0.01 to 5000 s^{-1} with 5 points per decade, each point was maintained for a duration of 180 s in order to perform measurements in the permanent regime. Data are the means of 3 analyses on different batches of the same type of formulations

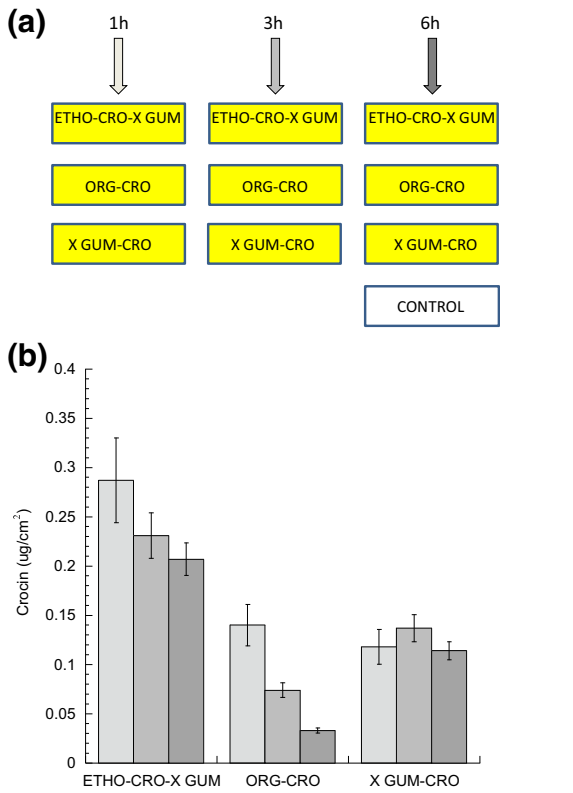

Fig. 5 Tape stripping evaluation. (**a**) Scheme of the forearm of the volunteers depicting the modality of application of the formulations. (**b**) CRO amount in the *stratum corneum* after ETHO-CRO-X GUM, ORG-CRO and X GUM-CRO application, removal and tape stripping. Tape stripping was performed after 1 ( ), 3 ( ), and 6 ( ) hours from the removal of formulations (**b**). Details are reported in the experimental section. Data represent the mean for ten subjects

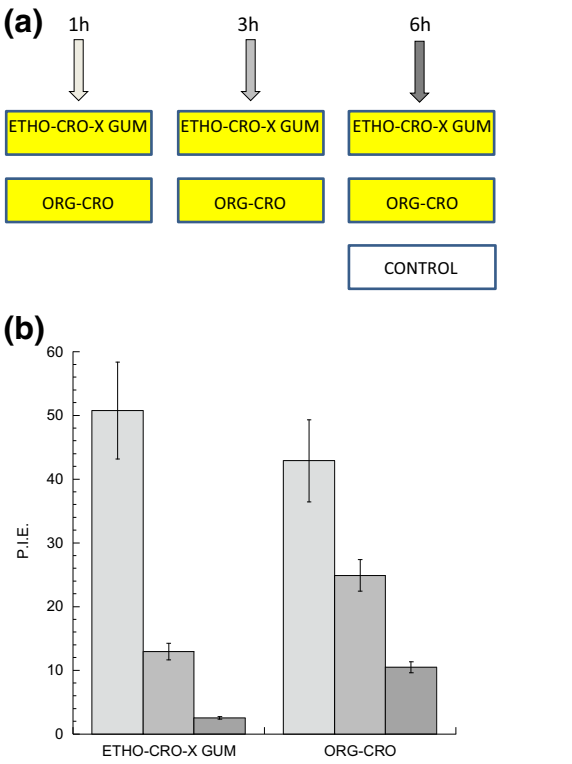

Fig. 6 Anti-inflammatory effect evaluation. (**a**) Scheme of the forearm of the volunteers depicting the modality of application of the formulations. (**b**) Variation of percentage of erythema index (P.I.E.) after topical application and removal of ETHO-CRO-X GUM and ORG-CRO. P.I.E. evaluation was performed after 1 ( ), 3 ( ), and 6 ( ) hours from the removal of formulations. Details are reported in the experimental section. Data represent the mean for ten subjects

CRO-X GUM, ORG-CRO and X GUM-CRO were significantly different.

3.7 *In vivo* anti-inflammatory activity

Since CRO can exert anti-inflammatory activity (Christodoulou et al. 2015; Nam et al. 2010), ETHO-CRO-X GUM and ORG-CRO were further investigated to determine their *in vivo* ability to inhibit the UVB-induced skin erythema. Skin reflectance spectrophotometry was used to determine the extent of the erythema and to assess the inhibition capacity of the formulations after their preventive application onto the skin. Figure 6a outlines the design of application of formulations on the forearm of volunteers. For each subject the AUC was determined plotting ΔEI values versus time. The PIE values reported in Fig. 6b indicate that after 1 h from the removal of formulations, ETHO-CRO-X GUM was more effective than ORG-CRO in inhibiting the induced erythema, while at 3 and 6 h ORG-CRO induced a higher inhibitory ability, respectively double and quadruple with respect to ETHO-CRO-X GUM ($p < 0.05$).

4 Discussion

In this study, in order to find cutaneous vehicles able to control CRO instability, different PC based nanosystems have been explored. The entrapment of the drug in ETHO and ORG has been spontaneously obtained upon addition of CRO solution to PC respectively solubilized in ethanol or in isopropylpalmitate. In both cases the production procedure did not imply heating or high energy input, avoiding in this way physico-chemical stresses towards the labile CRO molecule (Tsimidou and Tsatsaroni 1993).

The different supramolecular organization of PC resulted in the formation of spherical multilamellar vesicles in the case of ETHO-CRO or in an entanglement of extended worm-like reverse micelles in the case of ORG-CRO. Thus the former is an aqueous low viscous dispersion, while the latter is a w/o microemulsion with a viscosity depending on the amount of added water. As expected, in the case of ETHO-CRO, EC was not quantitative since the hydrophilic drug (log P -4.72) distributed partly in the aqueous environment outside the vesicles, contrarily ORG-CRO allowed complete entrapment of CRO in the aqueous domain inside the reverse

micelles. ETHO-CRO have been employed for *in vivo* studies as they were, with no separation of the amount of CRO out of the vesicles and without extrusion. Indeed the extrusion process resulted not only in a decrease of vesicle mean diameter, but also in a halving of CRO entrapment in the vesicles due to CRO leakage. Concerning ETHO-CRO mean diameter, it should be taken in consideration that the final gel formulations were designed for a cutaneous administration and not for a parenteral one, where mean diameter plays a fundamental role.

The peculiar CRO location has accounted for the different stabilizing power of ETHO-CRO and ORG-CRO, indeed in the case of ETHO-CRO the drug is partly distributed outside the vesicles and thus more exposed to chemical degradation, actually ORG-CRO was 5 fold more efficacious than ETHO-CRO in controlling CRO degradation. However both formulations remarkably controlled CRO stability with respect to plain solution, in fact it should be underlined that CRO in water was rapidly decomposed ($t_{1/2}$ 2.26 days) (Table 3).

ORG-CRO was constituted of PC 200 mM, a concentration effective for penetration enhancement, isopropylpalmitate, a biocompatible oil particularly suitable for transdermal delivery, and water (Fiume 2001; Changez et al. 2006). In ORG-CRO the reverse micelles initially formed, upon further addition of water linearly grew and entangled, finally constituting a three-dimensional network of interpenetrating worm-like micelles, stabilized by hydrogen bonds between PC and polar solvent molecules (Vintiloiu and Leroux 2008; Kumar and Katare 2005). While ORG-CRO possessed a viscosity suitable for cutaneous application, ETHO-CRO required an improvement of viscosity by direct X GUM addition.

Rheology studies evidenced a steady shear flow behaviour typical of X GUM dispersions for ETHO-CRO-X GUM (Song et al. 2006). Indeed it can be suggested that X GUM molecules aggregate through hydrogen bonding and polymer entanglement, leading to a high shear viscosity at low shear rates or at rest (Marcotte et al. 2001). The increase in shear rate caused a decrease of the steady shear viscosity since the polymer network disentangled and to individual macromolecules align in the shear flow direction, resulting in a low shear viscosity at high shear rate region. Shear removal resulted in reconstitution of network structure, rapidly recovering the viscosity (Vintiloiu and Leroux 2008). ETHO presence did not influence the rheology behaviour of ETHO X-GUM.

In the case of ORG-CRO the typical rheological behaviour of PC ORG was observed. Indeed, as previously found, the vehicles exhibited a Newtonian flow over the low shear rate range, with a near constant viscosity, suggesting that the micelle network did not break in this range (Schipunov and Hoffmann 2000; Hashizaki et al. 2008).

A further increment in shear rate led ORG-CRO to behave as a non-Newtonian fluid, displaying a decrease in viscosity. This behaviour could be attributed to a breakage of the micelle network structure provoked by the shear rate increment (Schipunov and Hoffmann 2000; Hashizaki et al. 2008).

CRO cutaneous biodistribution after application of ETHO-CRO-X GUM or ORG-CRO has been investigated by tape stripping and reflectance spectroscopy. The tapestripping technique allows direct quantification of drug amounts in the *stratum corneum*, while reflectance spectroscopy is able to give information about the concentration of CRO in the viable epidermis since it measures the anti-inflammatory effect due to CRO presence in the blood. In this respect the two methods can be considered complementary. In particular reflectance spectrophotometry monitores the degree of skin reddening. Before discussing the results, a brief methodological comment is in order. From reflectance spectra, generally in the range of 400–700 nm, the values of different colour space systems (CIELab, Lch, etc.) can be obtained using different International Commission on Illumination, CIE illuminants (C, D, A, etc.) and 2 or 10° illuminant observer. From spectral data it is possible to calculate at different wavelengths the relative reflectance or the logarithm of inverse reflectance (LIR), which is related to the light absorption of skin chromophores (hemoglobin, melanin, etc.). The EI obtained from skin reflectance spectral values is thought to give a more accurate and reliable evaluation of skin erythema (Harrison et al. 2004). Since this is due to an increased hemoglobin content in skin vessels, EI values are calculated by subtracting LIR values at 510 and 610 nm (mainly related to melanin absorbance) from the sum of LIR values at 540, 560, and 580 nm, the absorption peak wavelengths for hemoglobin.

CRO depletion profiles obtained by tape stripping suggested that both ETHO-CRO-X GUM and ORG-CRO enhanced the penetration of CRO with respect to X GUM. Nonetheless, the higher CRO amount found in the case of ETHO-CRO-X GUM could be justified the hypothesis of the formation of a PC depot in the stratum corneum from which CRO can be released in a controlled fashion (Esposito et al. 2014). Moreover it should be consider the heterogeneous distribution of CRO in ETHO-CRO-X GUM, indeed a portion of CRO is distributed in the multilamellar vesicles, while the unentrapped portion of CRO is free in the gel. Due to its heterogeneous distribution, CRO interact with the skin in different ways, resulting in a sustained presence in the *stratum corneum*.

Surprisingly, the profile obtained by reflectance spectroscopy evidenced an initial higher anti-inflammatory activity exploited by ETHO-CRO-X GUM, followed by a more pronounced decrease with respect to ORG-CRO. Notably, in the case of ETHO-CRO-X GUM, after 3 and 6 hs, CRO probably reached the dermal zone, afterwards the drug was rapidly removed by the blood stream. It

could be tentatively supposed that after 1 h from ETHO-CRO-X GUM removal, CRO could exert an intense anti-inflammatory activity due to the presence of a high amount of ethanol, acting as penetration enhancer (Harrison et al. 2004). Indeed ethanol is known to penetrate through intercellular lipids, increasing the cell membrane lipid fluidity and decreasing the density of lipid multilayer (Verma and Pathak 2010; Touitou and Godin 2007). However the higher enhancing effect of ETHO cannot be only due to the presence of ethanol, which is a permeability enhancer, but overall in the resulting drug carrier system as a whole. As suggested by other authors, it seems plausible that ETHO-CRO could form a colloidal film on the skin surface, this film would result in a reduction of skin dehydration and an impairment of the barrier properties (Bodade et al. 2013). In addition the well known flexibility of ETHO can also be a critical parameter (Mishra et al. 2013). Anyway both ETHO-CRO-X GUM and ORG-CRO were able to increase CRO penetration. Indeed it is reasonable to suppose a strong interaction of PC with the *stratum corneum* lipids (El Maghraby and Williams 2009; Satapathy et al. 2013) resulting in a high concentration of CRO in the vascularized section of the skin, where it displayed an anti-inflammatory activity.

5 Conclusions

ETHO and ORG have been demonstrated to be efficient vehicles for CRO administration on skin. Particularly ORG was able to better control CRO labile stability.

In vivo studies have demonstrated that thanks to the peculiar supramolecular organization of PC, both ETHO-CRO and ORG-CRO vehicles enhanced CRO absorption through skin, suggesting their suitability to treat inflammatory skin disorders. Moreover CRO can also have a protective effect on the surface of the skin, like sunscreens. This double effect could be useful for instance in melanoma prevention and therapy. Nonetheless, to verify this hypothesis animal studies should be performed.

Acknowledgments The authors are grateful to Sarah Villebrun from Institut Galien Paris-Sud, Châtenay-Malabry, France for rheological characterization.

Compliance with ethical standards

Ethical approval All procedures performed in studies involving human participants were in accordance with the 1964 Helsinki declaration and its later amendments or comparable ethical standards.

Informed consent Informed consent was obtained from all individual participants included in the study.

References

S.H. Alavizadeh, H. Hosseinzadeh, Bioactivity assessment and toxicity of crocin: a comprehensive review. Food Chem. Toxicol. **64**, 65–80 (2014)

A. Asai, T. Nakano, M. Takahashi, A. Nagao, Orally administered crocetin and crocins are absorbed into blood plasma as crocetin and its glucuronide conjugates in mice. J. Agric. Food. Chem. **53**, 7302–6 (2005)

S.S. Bodade, K.S. Shaikh, M.S. Kamble, P.D. Chaudhari, A study on ethosomes as mode for transdermal delivery of an antidiabetic drug. Drug Delivery **20**, 40–6 (2013)

M. Changez, J. Chander, A.K. Dinda, Transdermal permeation of tetracaine hydrochloride by lecithin microemulsion: in vivo. Colloids Surf. B: Biointerfaces **48**, 58–66 (2006)

E. Christodoulou, N.P. Kadoglou, N. Kostomitsopoulos, G. Valsami, Saffron: a natural product with potential pharmaceutical applications. J. Pharm. Pharmacol. **67**, 1634–49 (2015)

K.S. Chun, J. Kundu, J.K. Kundu, Y.J. Surh, Targeting Nrf2-Keap1 signaling for chemoprevention of skin carcinogenesis with bioactive phytochemicals. Toxicol. Lett. **229**, 73–84 (2014)

G.M. El Maghraby, A.C. Williams, Vesicular systems for delivering conventional small organic molecules and larger macromolecules to and through human skin. Expert Opin. Drug Deliv. **6**, 149–63 (2009)

J. Escribano, G.L. Alonso, M. Coca-Prados, J.A. Fernandez, Crocin, safranal and picrocrocin from saffron (Crocus sativus L.) inhibit the growth of human cancer cells in vitro. Cancer Lett. **100**, 23–30 (1996)

E. Esposito, R. Cortesi, M. Drechsler, L. Paccamiccio, P. Mariani, C. Contado, E. Stellin, E. Menegatti, F. Bonina, C. Puglia, Cubosome dispersions as delivery systems for percutaneous administration of indomethacin. Pharm. Res. **22**, 2163–73 (2005)

E. Esposito, P. Mariani, L. Ravani, C. Contado, M. Volta, S. Bido, M. Drechsler, S. Mazzoni, E. Menegatti, M. Morari, R. Cortesi, Nanoparticulate lipid dispersions for bromocriptine delivery: characterization and in vivo study. Eur. J. Pharm. Biopharm. **80**, 306–14 (2012)

E. Esposito, E. Menegatti, R. Cortesi, Design and characterization of fenretinide containing organogels. Mater. Sci. Eng. C **33**, 383–9 (2013)

E. Esposito, L. Ravani, P. Mariani, N. Huang, P. Boldrini, M. Drechsler, G. Valacchi, R. Cortesi, C. Puglia, Effect of nanostructured lipid vehicles on percutaneous absorption of curcumin. Eur. J. Pharm. Biopharm. **86**, 121–32 (2014)

Z. Fiume, Final report on the safety assessment of lecithin and hydrogenated lecithin. Int. J. Toxicol. **20**, 21–45 (2001)

B. Godin, E. Touitou, Ethosomes: new prospects in transdermal delivery. Crit. Rev. Ther. Drug Carrier Syst. **20**, 63–102 (2003)

J. Grdadolnik, J. Kidric, D. Hadzi, Hydration of phosphatidylcholine reverse micelles and multilayers-an infrared spectroscopic study. Chem. Phys. Lipids **59**, 57–68 (1991)

G.I. Harrison, A.R. Young, S.B. McMahon, Ultraviolet radiation-induced inflammation as a model for cutaneous hyperalgesia. J. Invest. Dermatol. **122**, 183–9 (2004)

K. Hashizaki, N. Tamaki, H. Taguki, Y. Saito, K. Tsuchiya, H. Sakai, M. Abe, Rheological behavior of worm-like micelles in a mixed nonionic surfactant system of a polyoxyethylene phytosterol and a glycerin fatty acid monoester. Chem. Pharm. Bull. **56**, 1682–6 (2008)

S. Jain, A.K. Tiwary, B. Sapra, N.K. Jain, Formulation and evaluation of ethosomes for transdermal delivery of lamivudine. AAPS PharmSciTech **8**, 249 E1–E9 (2007)

T. Konoshima, M. Takasaki, H. Tokuda, S. Morimoto, H. Tanaka, E. Kawata, L.J. Xuan, H. Saito, M. Sugiura, J. Molnar, Y. Shoyama, Crocin and crocetin derivatives inhibit skin tumor promotion in mice. Phytother. Res. **12**, 400–4 (1998)

R. Kumar, O.P. Katare, Lecithin organogels as a potential phospholipid-structured system for topical drug delivery: a review. AAPS PharmSciTech **6**, E298–310 (2005)

P.L. Luisi, R. Scartazzini, G. Haering, P. Schurtenberger, Organogels from water-in-oil microemulsions. Colloid Polym. Sci. **268**, 356–74 (1990)

M. Marcotte, R. Taherian Hoshahili, H.S. Ramaswamy, Rheological properties of selected hydrocol as a function of concentration and temperature. Food Res. Int. **34**, 695–703 (2001)

S.M. Meeran, M. Vaid, T. Punathil, S.K. Katiyar, Dietary grape seed proanthocyanidins inhibit 12-Otetradecanoyl phorbol-13-acetate-caused skin tumor promotion in 7,12-dimethylbenz[a]anthracene-initiated mouse skin, which is associated with the inhibition of inflammatory responses. Carcinogenesis **30**, 520–8 (2009)

A.D. Mishra, C.N. Patel, D.R. Shah, Formulation and optimization of ethosomes for transdermal delivery of ropinirole hydrochloride. Curr. Drug Deliv. **10**, 500–16 (2013)

A. Mittal, C.A. Elmets, S.K. Katiyar, Dietary feeding of proanthocyanidins from grape seeds prevents photocarcinogenesis in SKH-1 hairless mice: relationship to decreased fat and lipid peroxidation. Carcinogenesis **24**, 1379–88 (2003)

K.N. Nam, Y.M. Park, H.J. Jung, J.Y. Lee, B. Min, S. Park, W. Jung, K. Cho, J. Park, I. Kang, J. Hong, E.H. Lee, Anti-inflammatory effects of crocin and crocetin in rat brain microglial cells. Eur. J. Pharmacol. **648**, 110–6 (2010)

V. Nandakumar, T. Singh, S.K. Katiyar, Multi-targeted prevention and therapy of cancer by proanthocyanidins. Cancer Lett. **269**, 378–87 (2008)

K.D. Patil, S.R. Bakliwal, S.P. Pawar, Organogel: topical and transdermal drug delivery system. Int. J. Pharm. Res. Dev. **3**, 58–66 (2011)

R. Pecora, Dynamic light scattering measurement of nanometer particles in liquids. J. Nanopart. Res. **2**, 123–31 (2000)

W.J. Pugh, Kinetics of product stability, in *Aultons's Pharmaceutics. The design and manufacture of the medicines*, ed. by M.E. Aulton, 3rd edn. (Churchil Livingstone Elsevier, London, 2007), pp. 99–107

S. Raut, S.S. Bhadoriya, V. Uplanchiwar, V. Mishra, A. Gahane, S.K. Jain, Lecithin organogel: a unique micellar system for the delivery of bioactive agents in the treatment of skin aging. Acta Pharm. Sin. B **2**, 8–15 (2012)

F.M. Robertson, Skin carcinogenesis, in *Encyclopedia of cancer*, ed. by M. Schwab (Springer Berlin, Heidelberg, 2012), pp. 3432–5

D. Satapathy, D. Biswas, B. Behera, S.S. Sagiri, K. Pal, K. Pramanik, Sunflower-oil-based lecithin organogels as matrices for controlled drug delivery. J. Appl. Polym. Sci. **129**, 585–94 (2013)

Y.A. Schipunov, A micellar system with unique properties. Colloids Surf. A **185**, 541–54 (2001)

Y.A. Schipunov, H. Hoffmann, Thinning and thickening effects induced by shearing in lecithin solutions of polymer-like micelles. Rheol. Acta **39**, 542–53 (2000)

K.-W. Song, Y.-S. Kim, G.S. Chang, Rheology of concentrated xanthan gum solutions: Steady shear flow behaviour. Fibers Polym. **7**, 129–38 (2006)

Y.J. Surh, Cancer chemoprevention with dietary phytochemicals. Nat. Rev. Cancer **10**, 768–80 (2003)

W. Tian, Q. Hu, Y. Xu, Effect of soybean-lecithin as an enhancer of buccal mucosa absorption of insulin. Biomed. Mater. Eng. **22**, 171–8 (2012)

E. Touitou, B. Godin, Dermal drug delivery with ethosomes: therapeutic potential. Therapy **4**, 465–72 (2007)

E. Touitou, N. Dayan, L. Bergelson, B. Godin, M. Eliaz, Ethosomes-novel vesicular carriers for enhanced delivery: characterization and skin penetration properties. J. Control. Release **65**, 403–18 (2000)

M. Tsimidou, E. Tsatsaroni, Stability of saffron pigments in aqueous extracts. J. Food Sci. **58**, 1073–5 (1993)

P. Verma, K. Pathak, Therapeutic and cosmeceutical potential of ethosomes: an overview. J. Adv. Pharm. Technol. Res. **1**, 274–82 (2010)

A. Vintiloiu, J.-C. Leroux, Organogels and their use in drug delivery: a review. J. Control. Release **125**, 179–92 (2008)

H. Wanga, T.O. Khorb, L. Shu, Z. Su, F. Fuentes, J.-H. Lee, A.-N.T. Kong, Plants against cancer: a review on natural phytochemicals in preventing and treating cancers and their druggability. Anti Cancer Agents Med. Chem. **12**, 1281–305 (2012)

C.-J. Weng, G.-C. Yen, Chemopreventive effects of dietary phytochemicals against cancer invasion and metastasis: phenolic acids, monophenol, polyphenol and their derivatives. Cancer Treat. Rev. **38**, 76–87 (2012)

P. Winterhalter, R.M. Straubinger, Saffron, renewed interest in an ancient spice. Food Rev. Intl. **16**, 39–59 (2000)

J. Wohlrab, T. Klapperstück, H.W. Reinhardt, M. Albrecht, Interaction of epicutaneously applied lipids with stratum corneum depends on the presence of either emulsifiers or hydrogenated phosphatidylcholine. Skin Pharmacol. Physiol. **23**, 298–305 (2010)